JOURNAL OF THERMOPHYSICS AND HEAT TRANSFER
Vol. 21, No. 1, January–March 2007

Accurate Computations of Arc-Heater Flows Using Two-Equation Turbulence Models

Jeong-Il Lee,* Chongam Kim,† and Kyu-Hong Kim‡
Seoul National University, Seoul 151-742, Republic of Korea

DOI: 10.2514/1.25495

A new time marching solver, ARCFLO4, has been developed to analyze the flows in arc heaters. Governing equations are the hyperbolic-type axisymmetric Navier–Stokes equations including Joule heating, radiation, and turbulence models. To investigate the effect of turbulence models, k–ε, k–ω, and k–ω SST turbulence models are introduced into ARCFLO4. Throughout vast numerical calculations of the Aerodynamic Heating Facility and the Interaction Heating Facility at the NASA Ames Research Center, the k–ε turbulence model combined with the three-band radiation model exhibited good agreement with experiment data. In addition, it is confirmed that the turbulence effect plays a significant role in determining arc-heater flow physics.

Nomenclature

c = speed of light
B_ν = Plank function at frequency ν
E = voltage gradient
$\boldsymbol{E}$ = inviscid flux vector in the streamline direction
$\boldsymbol{E_v}$ = viscous flux vector in the streamline direction
$\boldsymbol{F}$ = inviscid flux vector in the radial direction
$\boldsymbol{F_v}$ = viscous flux vector in the radial direction
H = total enthalpy
$\boldsymbol{H}$ = axisymmetric inviscid source vector
H_a = mass-averaged enthalpy
$\boldsymbol{H_v}$ = axisymmetric viscous source vector
h = Planck's constant
I = current
$\boldsymbol{I}$ = Joule heating source vector
I_ν = specific radiative intensity
j = current density
k = Boltzmann constant
L = length of the constrictor
$\dot{m}$ = mass flow rate
p = pressure
$\boldsymbol{Q}$ = conservative variables vector
q_c = convective heat flux
q_n = radiative heat flux at frequency band
q_R = radiative heat flux
q_ν = radiative heat flux at frequency ν
R = radius of the constrictor
u = axial velocity
V = voltage
v = radial velocity
x = streamwise coordinate
y = radial coordinate
α = angle in the cross-sectional plane from the radial direction to the projected line of sight
η = arc-heater efficiency
θ = angle between the ray and the outward normal to the cylindrical surface
κ_ν = absorption coefficient
ν = radiation frequency
ρ = density
σ = electrical conductivity
τ_{ij} = shear stress
Ω = solid angle

I. Introduction

SINCE human beings stepped into space, numerous planetary entry vehicles have been developed to carry out various space missions. When entering the atmosphere of planets including the Earth, these vehicles are exposed to tremendous aerodynamic heating which necessitates some sort of thermal protection system (TPS). Thus, the TPS is regarded as one of the most important technologies in the design of planetary entry vehicle. Its importance is continuously increasing as reusable reentry vehicles are becoming more and more useful.

Keeping pace with space missions in Europe, Japan, and China, as well as USA, numerous ground test facilities have been developed. The most representative ground test facility for a TPS would be a plasma wind tunnel which can provide high enthalpy flows for a long time. Among several types of plasma wind tunnels, a segmented arc-heater wind tunnel can produce a stable and high-quality flow which is an essential requirement for ground experiments. Generally, flow in an arc heater is a complex plasma flow which is heated directly by arc. The flow experiences strong energy transfer from its core to the surrounding gas mainly by radiation and turbulence mixing. To unveil the flow physics, there have been many numerical and experimental investigations.

The present paper is concerned with numerical efforts to investigate the flow physics in an arc-heated wind tunnel. Historically, Nicolet et al. [1] developed the ARCFLO program based on the Waston and Pegot [2] study. It adopts a two-band radiation model that accounts for self-absorption and a Cebeci–Smith [3] algebraic turbulence model. The overall operating characteristics of existing arc heaters can be reasonably predicted. However, the characteristics of its radiation model are somewhat different from the real physical phenomena because the absorption coefficients for the radiation model are adjusted empirically by a long series of trials and errors. Thus, Sakai et al. [4,5] improved ARCFLO by changing the two-band radiation model into the PRG (Planck–Rosseland–Gray) radiation model which calculates a radiative heat flux using three mean absorption coefficients. This program could yield a fairly good agreement with experimental data by tuning a set of the turbulence parameters.

Received 30 May 2006; revision received 30 July 2006; accepted for publication 30 July 2006.

*Graduate Student, School of Mechanical and Aerospace Engineering, Sillim-Dong, Gwanak-Gu; snow0730@empal.com. Member AIAA.

†Professor, School of Mechanical and Aerospace Engineering and the Institute of Advanced Aerospace Technology, Sillim-Dong, Gwanak-Gu; chongam@snu.ac.kr. Member AIAA.

‡Assistant Professor, School of Mechanical and Aerospace Engineering and the Institute of Advanced Aerospace Technology, Sillim-Dong, Gwanak-Gu; aerocfd1@snu.ac.kr (corresponding author). Member AIAA.

These programs were developed commonly based on a space marching technique which requires the upstream conditions in advance. Thus, they are quite restrictive to be used in the design or development step of arc heaters. To overcome this deficiency, Kim et al. [6] developed the time marching code, ARCFLO2, which solves the hyperbolic-type Navier–Stokes equations. It calculated all of properties successfully only with a geometry of arc-heater and operating conditions: a current and a mass flow rate. Subsequently, Sakai and Olejniczak [7,8] made an attempt to improve ARCFLO2 and developed a new three-band radiation model which is almost consistent with the detailed line-by-line radiation calculation. Compared to the previous two-band radiation model, the new three-band radiation model is able to provide quite accurate solutions maintaining calculation efficiency.

Unfortunately, numerical codes developed so far do not guarantee sufficient numerical accuracy for various arc heaters under a wide range of operating conditions. This is because physical phenomena in an arc heater are too complex to be fully understood. Also, a numerical model cannot reflect them rightly. Roughly, the discrepancy between the real physics and computations would be attributed to the mispredicted heat transfer that mainly consists of radiative and convective heat transfers. Between two kinds of heat transfers, a radiative heat transfer is able to be calculated quite accurately. Especially, the three-band radiation model by Sakai and Olejniczak [8] is thought to be accurate and efficient enough in calculation of an arc heater. On the other hand, concerning a convective heat transfer, turbulence models that have been used in previous codes cannot provide the necessary level of accuracy until now. For example, solutions can be adjusted to experimental data for a specific arc heater by choosing a proper set of turbulence parameters and wall roughness or by directly controlling turbulence magnitude like additional numerical viscosity of ARCFLO2. However, if the same set of numerical parameters is applied to another arc heater, the accuracy cannot be guaranteed.

Keeping this in mind, we focused on the impact of turbulence models and developed the ARCFLO4 program, which can be applied to various arc heaters on arbitrary operating conditions. Instead of an algebraic turbulence model which was conventionally used, we adopted k–ε, k–ω, and k–ω SST two-equation turbulence models which are able to express the convective physics of turbulence and do not explicitly demand a mixing length. Then, they are applied to the Aerodynamic Heating Facility (AHF) and the Interaction Heating Facility (IHF) at the NASA Ames Research Center combined with the Joule heating model of ARCFLO [1] and the three-band radiation model of ARCFLO3 [8].

This paper is organized as follows: following introduction, Section I, governing equations, a Joule heating model, a radiation model, and turbulence models are briefly described in Section II, "Numerical Modeling." In the results section, Section III, the 20 MW AHF and the 60 MW IHF at the NASA Ames Research Center are calculated to verify a proper set of numerical models and the role of turbulent flow is investigated. Section IV is a discussion. Finally, concluding remarks, Section V, are presented based on numerous comparisons.

II. Numerical Modeling

A. Governing Equations

An arcjet wind tunnel is classified according to types of arc heaters. Figure 1 shows a segmented constrictor-type arc heater which is used worldwide. It consists of an anode chamber, a constrictor, a cathode chamber, and a nozzle. Most of the test gases are injected through the wall of the constrictor and exit through a nozzle into a test section. In a constrictor, the arc spans between the two electrodes. The core gas is heated by the arc's Joule heating. The surrounding gas is heated by radiation emitted from the core gas and by a turbulent mixing. Heat energy that arrives at the constrictor wall is removed by the cooling water which circulates through the constrictor disks.

For flow analysis, governing equations are chosen as the hyperbolic-type axisymmetric Navier–Stokes equations which include Joule heating by arc, radiation, and turbulence. They are written as follows in a vector form:

$$\frac{\partial \boldsymbol{Q}}{\partial t}+\frac{\partial \boldsymbol{E}}{\partial x}+\frac{\partial \boldsymbol{F}}{\partial y}+\boldsymbol{H}=\frac{\partial \boldsymbol{E}_v}{\partial x}+\frac{\partial \boldsymbol{F}_v}{\partial y}+\boldsymbol{H}_v+\boldsymbol{I} \tag{1}$$

where

$$\boldsymbol{Q}=\begin{bmatrix}\rho\\ \rho u\\ \rho v\\ \rho e_t\end{bmatrix},\qquad \boldsymbol{I}=\begin{bmatrix}0\\ 0\\ 0\\ -jE\end{bmatrix},\qquad \boldsymbol{H}=\frac{1}{y}\begin{bmatrix}\rho v\\ \rho uv\\ \rho v^2+p\\ \rho Hv\end{bmatrix}$$
$$\boldsymbol{H}_v=\frac{1}{y}\begin{bmatrix}0\\ \tau_{xy}\\ \tau_{yy}-\tau_{\theta\theta}\\ u\tau_{xy}+v\tau_{yy}-q_{c,y}-q_{R,y}\end{bmatrix} \tag{2}$$

$$\boldsymbol{E}=\begin{bmatrix}\rho u\\ \rho u^2+p\\ \rho uv\\ \rho Hu\end{bmatrix},\qquad \boldsymbol{F}=\begin{bmatrix}\rho v\\ \rho uv\\ \rho v^2+p\\ \rho Hv\end{bmatrix}$$
$$\boldsymbol{E}_v=\begin{bmatrix}0\\ \tau_{xx}\\ \tau_{xy}\\ u\tau_{xx}+v\tau_{xy}-q_{c,x}-q_{R,x}\end{bmatrix} \tag{3}$$
$$\boldsymbol{F}_v=\begin{bmatrix}0\\ \tau_{xy}\\ \tau_{yy}\\ u\tau_{xy}+v\tau_{yy}-q_{c,y}-q_{R,y}\end{bmatrix}$$

The gas is assumed to be in a chemical equilibrium state. Thermodynamic properties, such as pressure and temperature, and transport properties, such as viscosity and thermal conductivity, are calculated using curve-fitted data [9,10]. The available temperature range is up to 30,000 K, and the pressure range is 10^{-4}–10^{2} atm.

B. Numerical Schemes and Boundary Conditions

Governing equations are discretized using a finite volume method. The inviscid flux is given by the AUSMPW+ [11] scheme. The viscous flux is calculated through a central difference scheme. The inviscid term is handled implicitly by applying the Lower Upper Symmetric Gauss Seidel (LU-SGS). The axisymmetric source, Joule heating, and the viscous term are calculated explicitly.

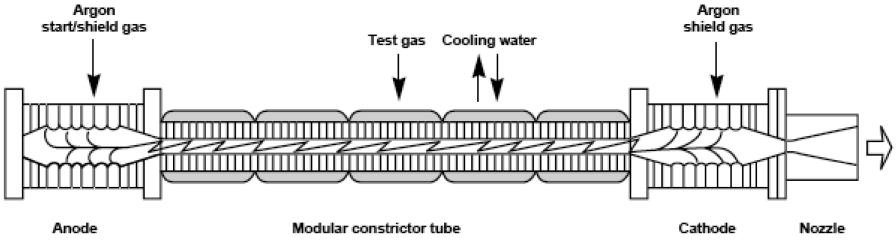

Fig. 1 Schematic drawing of a segmented arc heater.

For wall boundary conditions, air that is injected from gaps between adjacent constrictor disks is considered as a mass flow source distributed uniformly over the side wall [6]. Wall temperature is fixed at 1100 K and density at the wall is determined by the equilibrium relation between wall temperature and pressure [6]. The outlet condition is extrapolated from the value of the inner computational domain because the region after a nozzle throat is supersonic.

C. Joule Heating Modeling

Generally, Joule heating by arc should be obtained by solving Maxwell's equations. However, if the current distribution is known, it could be simply calculated by Ohm's law. Because the constrictor wall is insulated electrically, current in a constrictor is constant. Assuming that the voltage gradient is independent of radius, Joule heating can be simply calculated as follows.

Ohm's law for a cylindrical column is

$$j(x, y) = \sigma(x, y)E(x) \tag{4}$$

$$E(x) = \frac{j(x, y)}{\sigma(x, y)} = \frac{\int_0^R 2\pi y j(x, y)\,\mathrm{d}y}{\int_0^R 2\pi y \sigma(x, y)\,\mathrm{d}y} = \frac{I}{\int_0^R 2\pi y \sigma(x, y)\,\mathrm{d}y} \tag{5}$$

where

$$I = \int_0^R 2\pi y j(x, y)\,\mathrm{d}y = \text{const} \tag{6}$$

from Kirchhoff's law of conservation of current.

Finally, Joule heating is given as

$$j(x, y)E(x) = \frac{I^2\sigma(x, y)}{[\int_0^R 2\pi y \sigma(x, y)\,\mathrm{d}y]^2} \tag{7}$$

where the electrical conductivity is taken from [1]. Figure 2 shows the current distribution along the axial direction.

D. Radiation Modeling

For high temperature flows, radiation is an important heat transfer mode together with thermal convection. The radiative heat flux is calculated by the radiative transfer equation of Eq. (8).

$$-\frac{1}{\rho\kappa_\nu}\frac{\mathrm{d}I_\nu}{\mathrm{d}s} = I_\nu - B_\nu \tag{8}$$

where I_ν is the radiative intensity traveling along the ray s. The absorption coefficient is a function of frequency, temperature, and pressure, which is obtained from experiments. The Planck function is written as follows.

$$B_\nu = \frac{2h}{c^2}\frac{\nu^3}{e^{h\nu/kT} - 1} \tag{9}$$

When the radiative intensity at a given point is calculated for all directions, the radiant flux per unit frequency expressed in cylindrical coordinates can be calculated as (see Fig. 3)

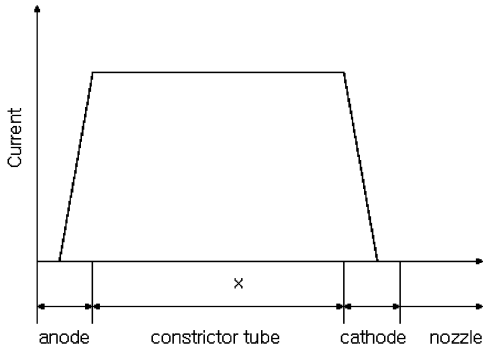

Fig. 2 Current distribution in the arc heater.

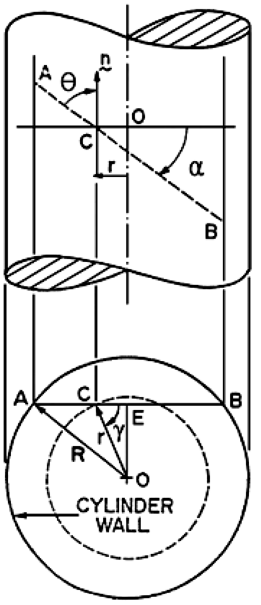

Fig. 3 Cylindrical geometry and coordinate system.

$$q_\nu(r) = \int_\Omega I_\nu(r)\cos\theta\,\mathrm{d}\Omega \tag{10}$$

The details can be found in [1]. The total radiant flux, integrated over all frequencies, is calculated as

$$q_R(r) = \int_0^\infty q_\nu(r)\,\mathrm{d}\nu \tag{11}$$

In a discrete form,

$$q_R(r) = \sum_n q_n(r) \tag{12}$$

To obtain accurate radiation, the line-by-line calculation [12] is most desirable. However, the computing cost for such a calculation is formidable. Thus, Sakai and Olejniczak [8] developed a new three-band model that can compute radiative transport equations 400 times faster than the detailed line-by-line calculation without compromising accuracy. In this model, three absorption coefficients, defined at a given wavelength, are functions of pressure and temperature over the pressure ranges from 1 to 10 atm and the temperature ranges from 1000 to 15,000 K. In the present work, we adopted the three-band radiation model [8] so as to accurately describe the radiative flow physics in arc heaters.

E. Turbulence Modeling

Turbulence is regarded as one of the key phenomena in an arc-heater flow. For its calculations, algebraic turbulence models have

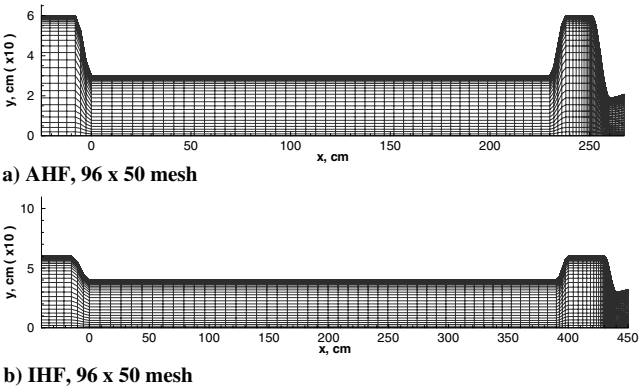

a) AHF, 96 x 50 mesh

b) IHF, 96 x 50 mesh

Fig. 4 Grid system.

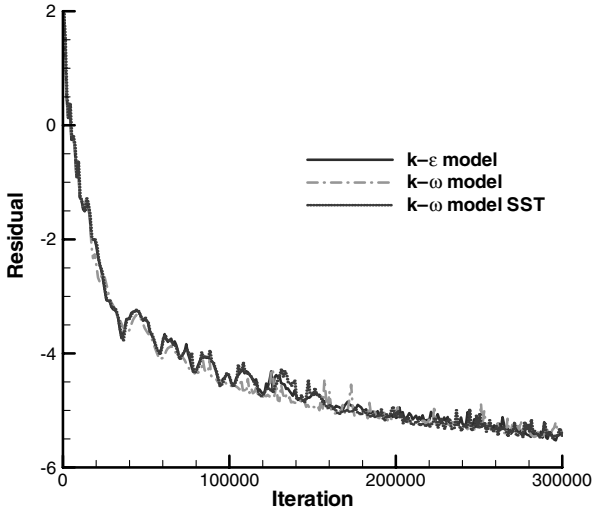

Fig. 5 Convergence history for the AHF grid ($I = 1600$ A, $\dot{m} = 0.45$ kg/s).

been used wherein the turbulent fluctuating quantities are correlated to the mean flow quantities by algebraic relations. They are the simplest to implement among all the available turbulence models and rarely cause unexpected numerical difficulties. However, they do not include the convection effect of turbulence [13] because they assume the local rate of turbulence production is approximately equal to the rate of turbulence dissipation. In addition, they cannot provide reasonable results once the turbulent mixing length is not accurate [14]. For these reasons, an accurate prediction is fairly limited. Unfortunately, in the case of arc-heated flow calculations, gas is injected perpendicularly through the constrictor wall and thus strong turbulence is induced, convected, and diffused along the main flow. Thus, it is almost impossible for coefficients of algebraic models to be tuned adequately for a wide range of arc-heater flows.

To overcome the deficiency, more advanced turbulence models which possess less empirical turbulence coefficients are introduced. In the present study, three two-equation turbulence models, i.e., the k–ε model of Jones and Launder [15], the k–ω model of Wilcox [14], and the k–ω SST model of Menter [16], were selected and their performances were examined. These are currently the most popular models that solve transport equations for turbulence kinetic energy. They can be used to predict properties of given turbulent flows without prior knowledge of turbulence structure. Depending on flow conditions, however, their performances are somewhat different from each other [17].

The k–ε model of Jones and Launder is the most well-known and extensively adopted two-equation eddy viscosity model. It is known that the model gives good agreement with experimental results for wall-bounded flows with zero or small mean pressure gradients, but it is less accurate for flows with large adverse pressure gradients. The k–ω model of Wilcox has proven to be superior in terms of numerical stability to the k–ε model primarily in the viscous sublayer near the wall. However, the results of the k–ω model are sensitive to the small freestream value of ω. The k–ω SST model of Menter combines several desirable features of the k–ε model and the k–ω model. This model becomes the k–ω model near a solid wall. It switches to the k–ε model near the boundary layer edges and in free-shear layers. The resulting shear stress transport (SST) modification accurately predicts flows with strong adverse pressure gradients and separation.

III. Results

In the present study, two-equation turbulence models and the three-band radiation model were coupled with the governing equations to accurately describe the mechanism of heat transfer in arc

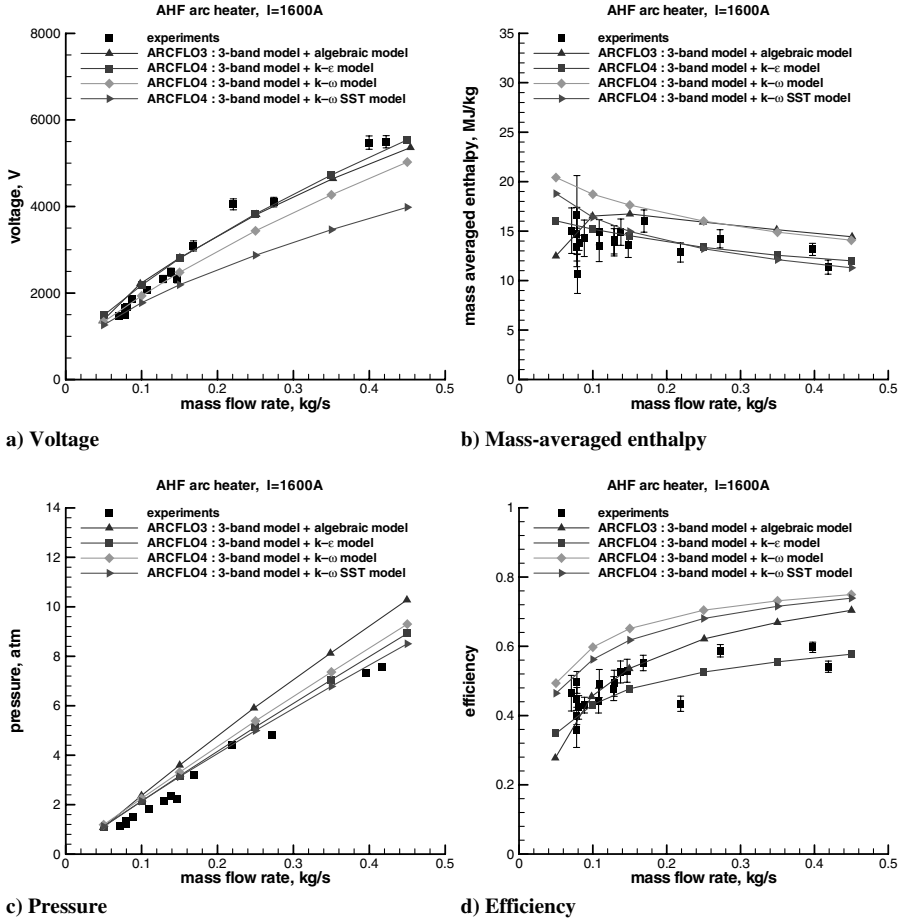

a) Voltage **b) Mass-averaged enthalpy**

c) Pressure **d) Efficiency**

Fig. 6 Comparisons between calculations and experiments (AHF, $I = 1600$ A).

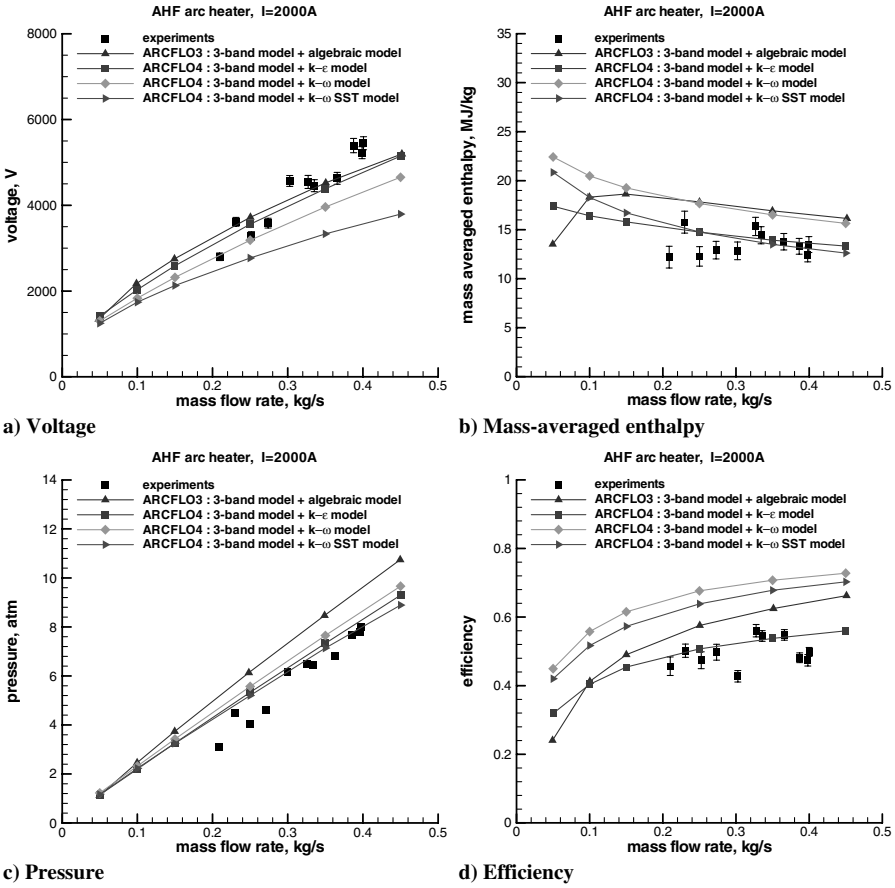

Fig. 7 Comparisons between calculations and experiments (AHF, $I = 2000$ A).

heaters. We carried out calculations for the following two sets of experimental data: data of the 20 MW AHF and the 60 MW IHF at the NASA Ames Research Center. After calculations, we compared basic performance parameters such as the voltage between electrodes, mass-averaged enthalpy at the nozzle throat, pressure in the cathode chamber, and arc-heater efficiency with the experimental data. Mass-averaged enthalpy and efficiency were defined as follows.

Mass-averaged enthalpy (J/kg):

$$H_a(x) = \frac{\int_0^R 2\pi y \rho(x,y) u(x,y) H(x,y)\,\mathrm{d}y}{\int_0^R 2\pi y \rho(x,y) u(x,y)\,\mathrm{d}y} \tag{13}$$

Efficiency (%):

$$\eta = \frac{\text{power absorbed by flow}}{\text{power input}} = 100 \times \left(1 - \frac{q_R - q_c}{IV}\right) \tag{14}$$

The dimensions of the constrictor and nozzle throat were directly obtained from [8]. The geometry of electrode chambers, which was not explicitly described in [8], was obtained by digitizing points of the scanned grid images. The AHF arc heater has a constrictor diameter of 0.06 m and a length of 2.3 m. The nozzle throat diameter is 0.038 m. The IHF arc heater has a constrictor diameter of 0.08 m, a length of 3.9 m, and a nozzle throat of 0.0603 m. The computational grids which are scaled up to 10 times in the radial direction are shown in Fig. 4.

The residual history for the AHF is shown in Fig. 5. It was observed that the residual reduced to 10^{-5} for all turbulence models. In addition, grid convergence tests were performed to validate the results. Even with a finer grid system, results varied within about 1% difference in the basic performance parameters.

A. Comparison with the AHF Data

The AHF is operated with a 20 MW constricted arc heater which produces a pressure range of 1–9 atm and an enthalpy level of 1–33 MJ/kg. Recently, Hightower et al. [18] carried out a series of arcjet tests in the AHF using the energy balance method. Sakai and Olejniczak [8] computed those flows using ARCFLO3 and compared the computed results with Hightower's experimental data.

In the present study, the comparison between computations and experiments was made for the AHF arc heater in a similar manner as Sakai and Olejniczak's study. Calculated voltage, mass-averaged enthalpy, chamber pressure, and efficiency were compared with experiment data for the cases of $I = 1600$ and 2000 A, respectively. The data were plotted in terms of mass flow rates. Figure 6 shows results for $I = 1600$ A. Calculated results using the k–ε turbulence model seemed to be the most accurate. The distribution of mass-averaged enthalpy and efficiency agreed especially well with experimental data. In the case of the k–ω turbulence model and k–ω SST turbulence model, qualitative trend matched with experiments but much of the calculated data, except for pressure, deviated from the experimental data. The k–ω turbulence model overestimated the mass-averaged enthalpy and efficiency for all mass flow rates. The k–ω SST turbulence model predicted lower voltage and higher efficiency. Figure 7 shows the results for $I = 2000$ A. Overall results exhibited a similar tendency to the case of $I = 1600$ A. Among the three different turbulence models, the k–ε turbulence model yielded the most accurate results again.

Based on the computations for the AHF arc heater, we concluded that the results were quite sensitive to the selection of turbulence model. Also, computations showed that the k–ε turbulence model predicted the overall flow characteristics of the AHF most accurately among tested models.

B. Comparison with the IHF Data

The IHF is equipped with a 60 MW constricted arc heater that operates at a pressure range of 1–9 atm and an enthalpy level of

7–47 MJ/kg. Arcjet tests in the IHF were performed by Hightower et al. The flows were computed by Sakai and Olejniczak [8].

As in the preceding section, we compared calculated results with experimental data as well as the data calculated by Sakai and Olejniczak. The results were presented for the cases of $I = 3000$ and 6000 A, respectively. Figure 8 shows calculated and experimental data for $I = 3000$ A. Similar to the results of the AHF, the k–ε turbulence model predicted voltage, mass-averaged enthalpy, chamber pressure, and efficiency accurately. Most computed data were within the range of the error bar of experimental data, and only a small amount of the computed data exhibited small differences. In the case of the k–ω turbulence model, voltage and chamber pressure were predicted accurately whereas mass-averaged enthalpy and efficiency were overestimated. In the case of the k–ω SST turbulence model, mass-averaged enthalpy and chamber pressure were predicted fairly well but voltage and efficiency were somewhat deviated. Figure 9 shows the results for $I = 6000$ A. Again, the overall results showed the same tendency as in the case of $I = 3000$ A. As shown in the figures, calculated results using the k–ε turbulence model agreed very well with the experimental data. On the other hand, some results with the k–ω turbulence model and k–ω SST turbulence model produced noticeable differences from experimental data.

Based on Figs. 6–9, the combination of the k–ε turbulence model and the three-band radiation model seems to provide accurate performance parameters of arc heater. Notably, a numerical solution in the present approach does not require a user's experience on turbulent flows different from the previous algebraic turbulence model. In this sense, the present numerical approach can be applied to a wide range of arc heaters. It can provide reasonable numerical results without prior knowledge on the arc-heater characteristics.

C. Comparison of Heat Flux Between Turbulence Models

To investigate quantitative differences among the three turbulence models, turbulent viscosity and turbulent heat flux were compared according to turbulence models. Figures 10 and 11 show distributions of turbulent viscosity and turbulent heat flux in the radial direction at the end of the AHF and the IHF constrictor. Judging from Figs. 6–9, accurate prediction of mass-averaged enthalpy and efficiency seems to be most difficult. The k–ε model provides quite reasonable results whereas the k–ω and k–ω SST turbulence models are somewhat overpredictive. From this point of view, the turbulent viscosity obtained by the k–ε model is physically more meaningful. In Fig. 10, it is seen that the k–ω and k–ω SST turbulence models underestimate turbulent viscosities and turbulent heat fluxes along the radial direction. As a result, the loss by thermal conduction decreases at the wall and the mass-averaged enthalpy and efficiency are relatively higher than the results from the k–ε turbulence model and experimental data as shown in Figs. 6b and 6d. This tendency is observed again for the IHF as shown in Figs. 8a, 8d, and 11.

D. Comparison of Heat Transfer Between Radiation and Turbulence

Flow characteristics in an arc heater critically depend on the heat transfer mechanism from the core to the surrounding. It is well known that most of the heat energy is transferred by radiation and turbulent phenomena. We compared the heat absorption by radiation and turbulence to check the influence of turbulence on a flow in an arc heater. Figure 12 shows the heat flux with the k–ε model along the radial direction at the beginning, the middle, and the end section of a constrictor. The heat absorption in a cell was calculated from the difference of energy fluxes at cell-interfaces. Thus, the negative gradient in Figs. 12 and 13 indicates that the gas absorbs heat energy

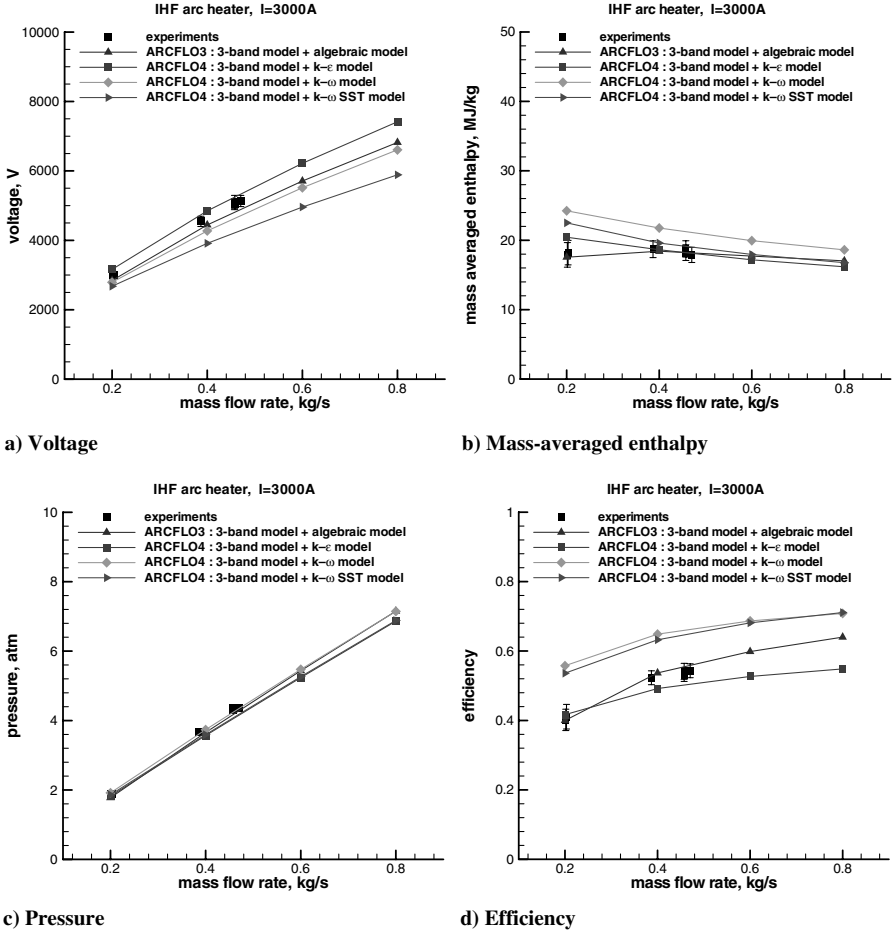

a) Voltage

b) Mass-averaged enthalpy

c) Pressure

d) Efficiency

Fig. 8 Comparisons between calculations and experiments (IHF, $I = 3000$ A).

whereas the positive gradient means emission or loss of heat energy. In Fig. 12a, at the beginning section of the constrictor, the radiative heat flux is bigger than the turbulent heat flux. In the core region, gas emits a large amount of heat energy by radiation. The energy is absorbed by the surrounding gas or transferred to the constrictor wall. However, at the middle section of constrictor (see Fig. 12b), the heat absorption and loss by turbulence are larger than those by radiation. From Figs. 12a and 12b, it is seen that the heat absorption and loss by radiation tend to decrease whereas those by turbulence tend to increase. In Fig. 12c, the amount of the radiative heat absorption and loss is quite small and most of heat transfer is realized by turbulence. Consequently, as the flow convects on the downstream side, radiation effect tends to weaken whereas turbulence effect tends to intensify. As shown in Fig. 13, this phenomenon becomes more evident as the mass flow rate injected from the wall increases. This confirms that the influence of turbulence on heat transfer mechanism is as much as or bigger than the radiation effect.

E. Comparison of Centerline Enthalpy

At the test section of arcjet facility, enthalpy is highest at the core, and it decreases gradually along the outer region near wall. Because actual arcjet experiments are carried out around the core region, the centerline enthalpy is an important physical parameter.

Fletcher and Bamford [19] measured the centerline enthalpy in the AHF using a laser-induced fluorescence method. They obtained two sets of experimental data at two different nominal constrictor chamber pressures, 2.4 and 4.8 atm. These experimental data are compared with computed results using the k–ε turbulence model. Figures 14 and 15 show the results: one for lower pressure case with the mass flow rate of 0.11 kg/s and the other for higher pressure case with the mass flow rate of 0.2 kg/s, respectively. It is seen that all of data calculated by the k–ε turbulence model are within the error bar of the experimental data. Based on these calculated results, the ratio of centerline enthalpy to mass-averaged enthalpy is between 1.12 and 1.14.

Park et al. [20] determined the mass-averaged enthalpy in the IHF by the heat balance method and the sonic throat method, and also measured the centerline enthalpy by the heat transfer rate method and the spectrometric method. As the operating conditions of these tests, the mass flow rate was 0.412 kg/s and the electrical current was maintained at an averaged value of 6066 A. The mean value of the mass-averaged enthalpy between the heat balance method and the sonic throat method was 28.8 MJ/kg. The lower bound of the centerline enthalpy determined by the heat transfer rate method was 30.5 MJ/kg. The spectrometric method resulted in a centerline enthalpy of 40.6 MJ/kg. The ratios of centerline enthalpy to mass-averaged enthalpy were 1.06 and 1.41, respectively. In the present study, the computation yielded the mass-averaged enthalpy of 27.1 MJ/kg and the centerline enthalpy of 32.9 MJ/kg at the nozzle throat. The ratio of centerline enthalpy to mass-averaged enthalpy was determined 1.21, which was a value between the heat transfer rate method and the spectrometric method.

Even though they were within the error bar of the experimental data, the calculated values of centerline enthalpy seem to be underestimated to some extent. It may be due to the excessive turbulence effect on the core region or no consideration of the electromagnetic force, i.e., the Lorentz force. With consideration of the MagnetoHydroDynamics (MHD) effect, a plasma flow is expected to be driven into the centerline by the Lorentz force. Accordingly, the arc radius would decrease and the centerline enthalpy increase.

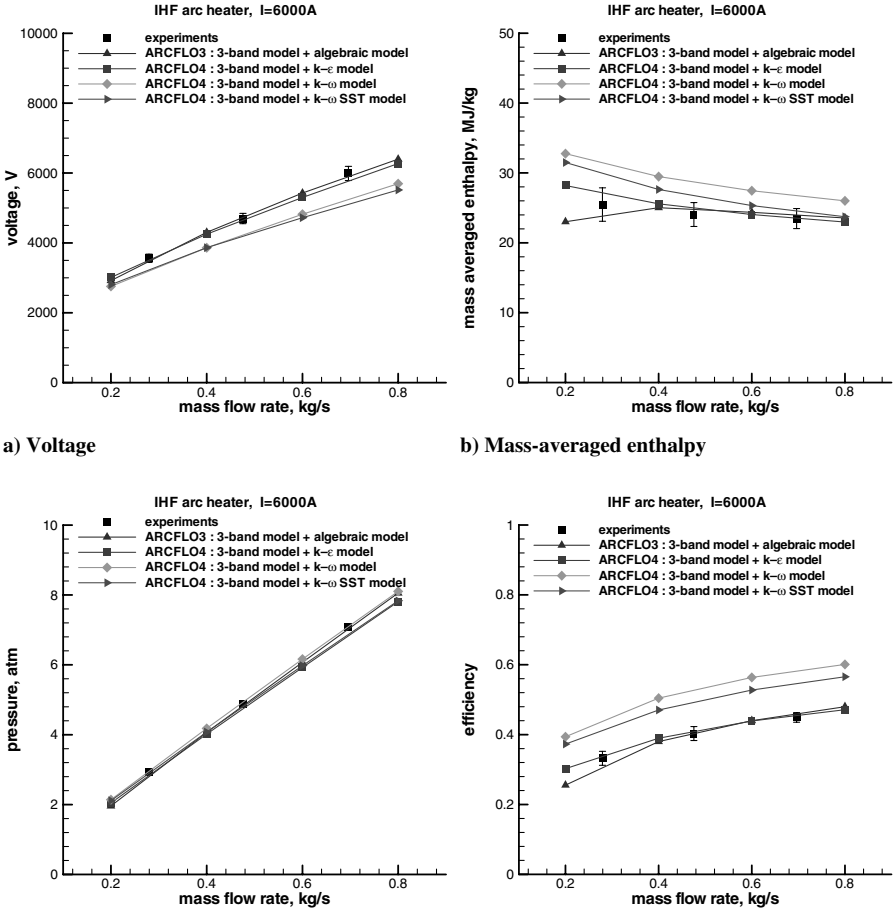

a) Voltage

b) Mass-averaged enthalpy

c) Pressure

d) Efficiency

Fig. 9 Comparisons between calculations and experiments (IHF, $I = 6000$ A).

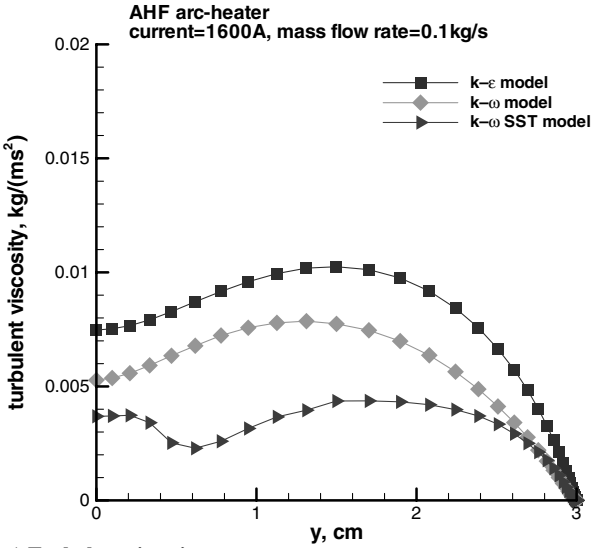

a) Turbulent viscosity

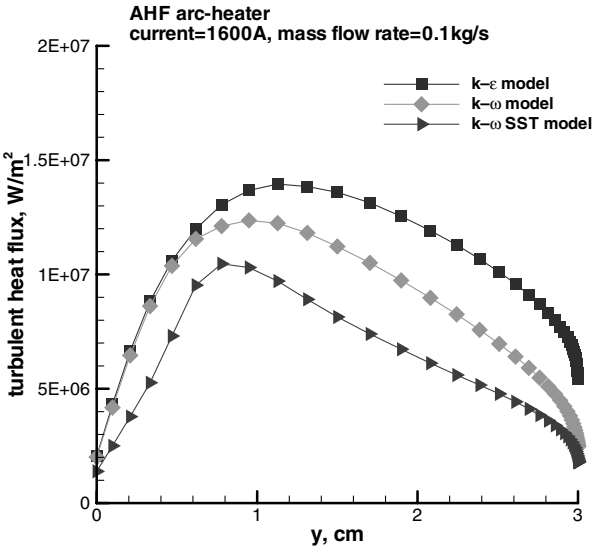

b) Turbulent heat flux

Fig. 10 Comparisons between turbulence models (AHF).

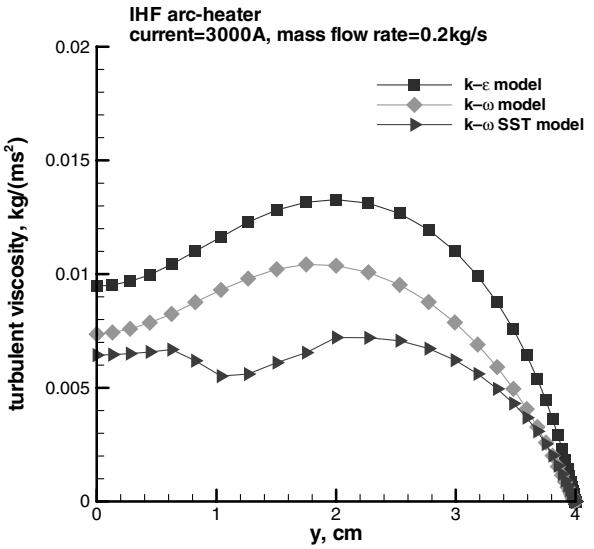

a) Turbulent viscosity

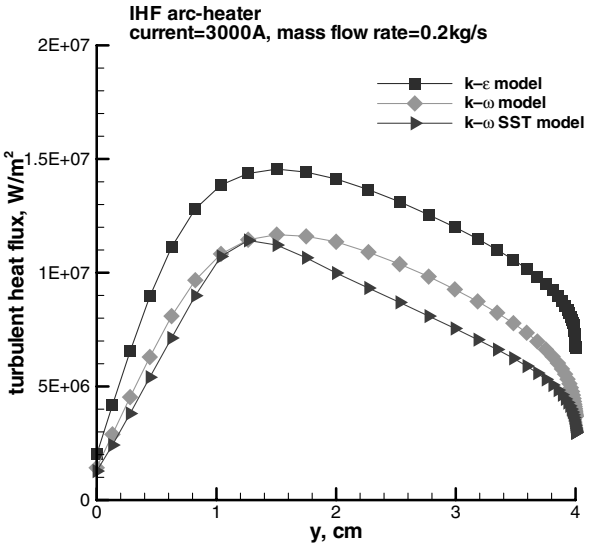

b) Turbulent heat flux

Fig. 11 Comparisons between turbulence models (IHF).

IV. Discussion

Based on comparisons between experiments and computations, it is reasonable to say that the k–ε turbulence model combined with the three-band radiation model provides quite good solutions under diverse operating conditions. However, in some regions, especially in the low mass flow rate condition of the AHF, accuracy of mass-averaged enthalpy does not seem to be guaranteed. The decrease of credibility of calculations may be caused by the ignorance of argon injection in the electrodes. Generally, a small amount of argon gas, e.g., about 0.03 kg/s in the AHF and 0.04 kg/s in the IHF, should be injected in electrodes to ensure that sufficient ionizations are maintained near the surface of the electrodes. However, the present study ignored the effect of argon gas because the mass flow rate of air was large enough in most test cases of the present paper. Accordingly, it is much probable that the solution is affected by the small amount of argon gas if the mass flow rate of air decreases below 0.1 kg/s, i.e., the order of mass flow rate of air becomes similar to that of argon gas. As shown in Figs. 6b and 7b, the discrepancy of the mass-averaged enthalpy between the present results and Sakai and Olejniczak's results [8] at low mass flow rate is apparent, especially less than 0.1 kg/s. If the argon gas is considered, it is expected that the mass-averaged enthalpy would follow the tendency of Sakai and Olejniczak's results.

Another important factor that should be investigated carefully is the current distribution in the electrode chambers, especially in the cathode chamber. It was observed from our results that the voltage was highly influenced by the shape of cathode and the distribution of current. Also, efficiency and mass-averaged enthalpy were influenced. From the fact that ARCFLO4 is well predicting the flow physics in arc heaters, our assumption that current decreases linearly in cathode region looks reasonable in most computations. However, some other current distribution could provide the better solution in a specific case. Thus, as one of the future works, the separate research on the cathode region seems to be necessary by introducing MHD.

Lastly, for the closer simulations to real phenomena, the effect of the wall boundary condition has to be investigated in detail. In a real arc-heater flow, gas is injected inclinedly from several points on the constrictor wall, which makes a flow swirling. Accordingly, the velocity of the injected gas flow is expected to be much higher than that of our uniform injection model and the strength of turbulence also become stronger. Therefore, even though the k–ε model provided the best solutions under the present models and assumptions, it is thought that an appropriate turbulence model should be selected again if the real injection environment is taken into account.

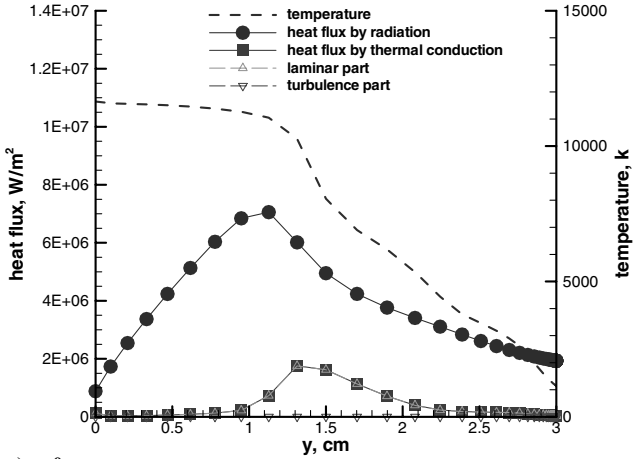

a) x=0

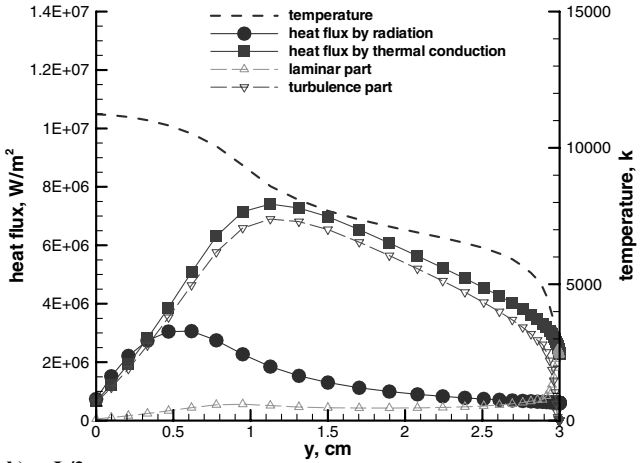

b) x=L/2

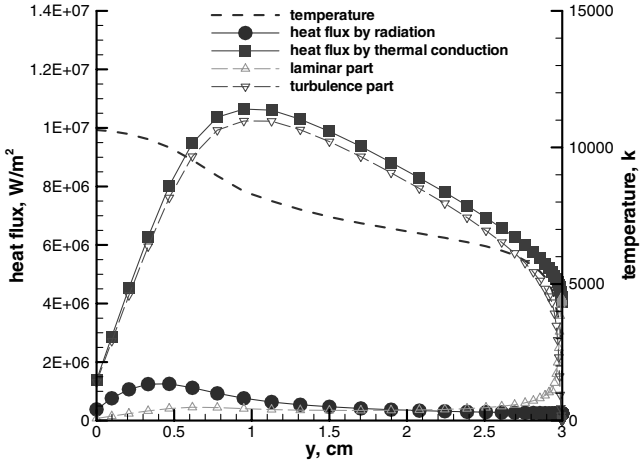

c) x=L

Fig. 12 Heat transfer mechanism in the constrictor (AHF, $I = 1600$ A, $\dot{m} = 0.1$ kg/s).

Although the nonequilibrium effect of electron temperature has been considered as one of the important factors to be investigated more, it is not discussed in the present paper because many researcher have already mentioned it [6–8].

V. Conclusions

The major objective of the work described in the present paper has been to find the proper turbulence model for accurate analysis of flow in arc heaters. Key physical phenomena in an arc heater were determined by the relative magnitude of Joule heating by arc, radiation, and turbulence. In the present code, ARCFLO4, Joule heating was simply calculated by Ohm's law with the given distribution of current. Radiation was computed by the three-band model which was almost consistent with the detailed line-by-line

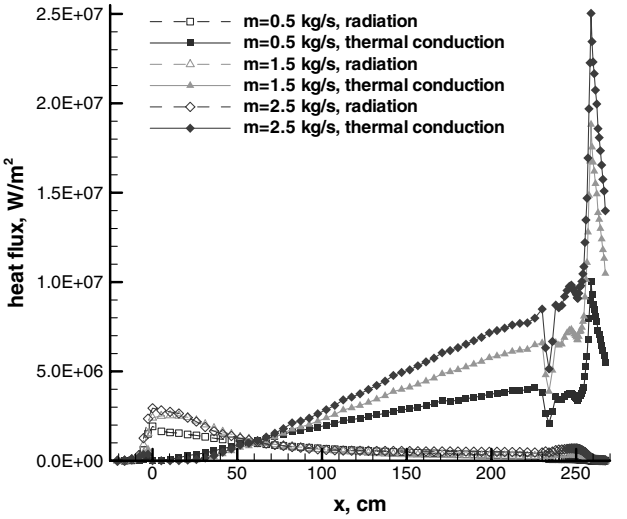

Fig. 13 Comparison of heat flux at the wall of the arc heater (AHF, I = 1600 A).

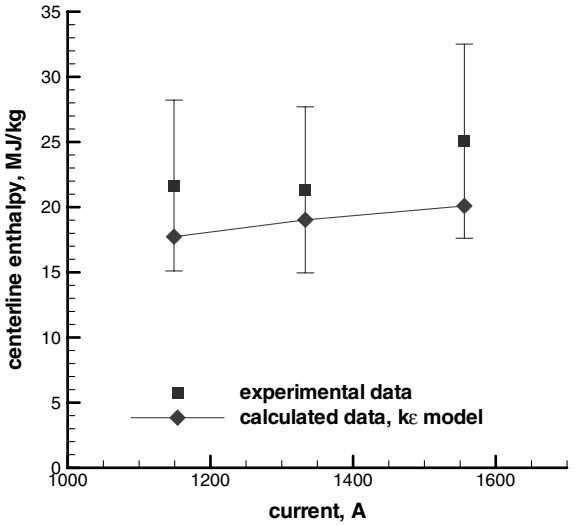

Fig. 14 Centerline enthalpy for the AHF (2.4 atm).

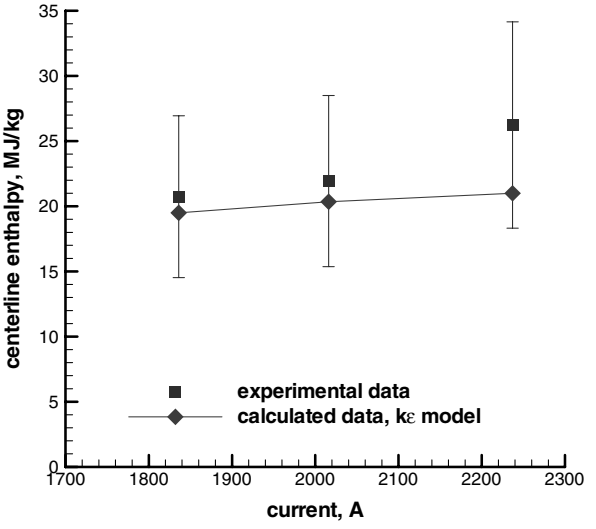

Fig. 15 Centerline enthalpy for the AHF (4.8 atm).

radiation model. Several two-equation turbulence models, the k–ε, k–ω, and k–ω SST turbulence models were adopted to investigate the impact of turbulence models. With the present code, the flow analysis of the 20 MW Aerodynamic Heating Facility and the 60 MW Interaction Heating Facility at the NASA Ames Research Center was conducted. It was observed that the k–ε turbulence model combined with the three-band radiation model was the most appropriate in analyzing flow physics of arc heaters. In addition, because it did not require a user's experience on turbulent flows, it showed the possibility of numerical design of arc heaters. Through comparisons between the radiative and turbulent heat fluxes, it was shown that the influence of turbulence on the heat transfer mechanism was as much as or bigger than that of radiation. An accurate turbulence model was one of the key factors in predicting arc heater performances.

Acknowledgments

This work was supported by grant No. R01-2006-000-10034-0 from the Basic Research Program of the Korea Science & Engineering Foundation. Additionally, the authors also appreciate the financial support from the Brain Korea 21 Project. The authors would like to specially thank Takehara Sakai for an offer of his three-band radiation code at the Nagoya University. The authors would like to also thank Chul Park for a technical guidance at the Korea Advanced Institute of Science and Technology. The authors would like to acknowledge the support from KISTI (Korea Institute of Science and Technology Information) under the Strategic Supercomputing Support Program with Sang Min Lee as the technical supporter. The use of the computing system of the Supercomputing Center is also greatly appreciated.

References

[1] Nicolet, W. E., Shepard, C. E., Clark, K. J., Balakrishnan, A., Kesselring, J. P., Suchsland, K. E., and Reese, J. J., "Analytical and Design Study for a High-Pressure, High-Enthalpy Constricted Arc Heater," Arnold Engineering Development Center, AEDC-TR-75-47, July 1975.

[2] Watson, V. R., and Pegot, E. B., "Numerical Calculations for the Characteristics of a Gas Flowing Axially Through a Constrictor Arc," NASA TN D-4042, June 1967.

[3] Smith, A. M. O., and Cebeci, T., "Numerical solution of the turbulent boundary layer equations," Douglas Aircraft Division Report DAC 33735, May 1967.

[4] Sakai, T., Sawada, K., and Park, C., "Assessment of Planck-Rosseland-Gray Model for Radiation Shock Layer," AIAA Paper 97-2560, June 1997.

[5] Sakai, T., Sawada, K., and Mitsuda, M., "Application of Planck-Rosseland-Gray Model for High Enthalpy Arc Heaters," *Journal of Thermophysics and Heat Transfer*, Vol. 15, No. 2, 2001, pp. 176–183.

[6] Kim, K. H., Rho, O. H., and Park, C., "Navier-Stokes Computation of Flows in Arc Heaters," *Journal of Thermophysics and Heat Transfer*, Vol. 14, No. 2, 2000, pp. 250–258.

[7] Sakai, T., and Olejniczak, J., "Navier-Stokes Computations for Arcjet Flows," AIAA Paper 2001-3014, June 2001.

[8] Sakai, T., and Olejniczak, J., "Improvement in a Navier-Stokes Code for Arc Heater Flows," AIAA Paper 2003-3782, June 2003.

[9] Srinivasan, S., Tannehill, J. C., and Weilmuenster, K. J., "Simplified Curve Fits for the Thermodynamic Properties of Equilibrium Air," NASA RP-1181, Aug. 1987.

[10] Gupta, R. N., Lee, K. P., Thompson, R. A., and Yos, J. M., "Calculations and Curve Fits of Thermodynamics and Transport Properties for Equilibrium Air to 30000 K," NASA RP-1260, Oct. 1991.

[11] Kim, K. H., Kim, C., and Rho, O. H., "Methods for the Accurate Computations of Hypersonic Flows: 1. AUSMPW + Scheme," *Journal of Computational Physics*, Vol. 174, Nov. 2001, pp. 38–80.

[12] Whiting, E. E., Park, C., Liu, Y., Arnold, J. O., and Paterson, J. A., "NEQAIR96, Nonequilibrium and Equilibrium Radiative Transport and Spectra Program: User Manual," NASA Reference Publication 1389, Dec. 1996.

[13] Hoffmann, K. A., and Chiang, S. T., "Computational Fluid Dynamics Volume III," *Zero-Equation Turbulence Model*, 4th ed., Engineering Education System, Wichita, KS, 2000, pp. 39–42.

[14] Wilcox, D. C., "Turbulence Modeling for CFD," *The k–ε Model*, 2nd ed., DCW Industries, La Canada, CA, 1998, pp. 119–122.

[15] Jones, W. P., and Launder, B. E., "The Prediction of Laminarization with a Two-Equation Model of Turbulence," *International Journal of Heat and Mass Transfer*, Vol. 15, No. 2, 1972, pp. 301–314.

[16] Menter, F. R., "Two-Equation Eddy Viscosity Turbulence Models for Engineering Applications," *AIAA Journal*, Vol. 32, Nov. 1994, pp. 1299–1310.

[17] Bardina, J. E., Huang, P. G., and Coakley, T. J., "Turbulence Modeling Validation, Testing, and Development," NASA Technical Memorandum 110446, April 1997.

[18] Hightower, T. M., Balboni, J. A., MacDonald, C. L., Anderson, K. F., and Martinez, E. R., "Enthalpy by Energy Balance for Aerodynamic Heating Facility at NASA Ames Research Center Arc Jet Complex," *48th International Instrumentation Symposium, the Instrumentation, Systems, and Automation Society* , Research Triangle Park, NC, May 2002.

[19] Fletcher, D. G., and Bamford, D. J., "Arcjet Flow Characterization Using Laser-Induced Fluorescence of Atomic Species," AIAA Paper 98-2458, June 1998.

[20] Park, C., Raiche, G. A., Driver, D. M., Olejniczak, J., Terrazas-Salinas, I., Hightower, T. M., and Sakai, T., "Comparison of Enthalpy Determination Methods for an Arc-Jet Facility," AIAA Paper 2004-487, Jan. 2004.